Structural Engineering and Mechanics, *Vol. 67, No. 1 (2018) 45-52*
DOI: https://doi.org/10.12989/sem.2018.67.1.045

Experimental investigation on optimal shear strengthening of RC beams using NSM GFRP bars

M. Ramezanpour[a], R. Morshed* and A. Eslami[b]

Department of Civil Engineering, Yazd University, Yazd, Iran

(Received May 10, 2017, Revised March 30, 2018, Accepted April 18, 2018)

Abstract. Several techniques have been developed for shear strengthening of reinforced concrete (RC) members by using fiber reinforced polymer (FRP) composites. However, debonding of FRP retrofits from concrete substrate still deemed as a challenging concern in their application which needs to be scrutinized in details. As a result, this paper reports on the results of an experimental investigation on shear strengthening of RC beams using near surface mounted (NSM) FRP reinforcing bars. The main objective of the experimentation was increasing the efficiency of shear retrofits by precluding/postponing the premature debonding failure. The experimental program was comprised of six shear deficient RC beams. The test parameters include the FRP rebar spacing, inclination angle, and groove shape. Also, an innovative modification was introduced to the conventional NSM technique and its efficiency was evaluated by experimental observation and measurement. The results testified the efficiency of glass FRP (GFRP) rebars in increasing the shear strength of the test specimens retrofitted using conventional NSM technique. However, debonding of FRP bars impeded exploiting all retrofitting advantages and induced a premature shear failure. On the contrary, application of the proposed modified NSM (MNSM) technique was not only capable of preventing the premature debonding of FRP bars, but also could replace the failure mode of specimen from the brittle shear to a ductile flexural failure which is more desirable.

Keywords: RC beam; shear strengthening; GFRP rebars; debonding; NSM; modified NSM

1. Introduction

One of the major applications of fiber reinforced polymer (FRP) composites is for shear strengthening of deficient reinforced concrete (RC) members. Over the past two decades, shear and/or flexural strengthening with externally bonded FRP laminates have become a renowned and promising technique owing to extensive experimental tests (Chajes *et al.* 1994, Khalifa *et al.* 1998, Mosallam and Banerjee 2007, Kocak *et al.* 2007, Eslami and Ronagh 2014, Onal *et al.* 2014, Mostofinejad and mahmoudabadi 2010, Mahini and Ronagh 2010, Anil *et al.* 2010), analytical investigations (Teng *et al.* 2007, Teng and Tedesco 2000, Dalalbashi *et al.* 2012, Deng *et al.* 2016, Kocak 2015) , and nonlinear finite element models (Dalalbashi *et al.* 2012, Baji *et al*. 2015, Dalalbashi *et al.* 2013) conducted in the field. Near surface mounted (NSM) technique has been also introduced as a more efficient alternative in FRP strengthening of RC beams (Dias and Barros 2013, Bianco *et al.* 2014). In this technique, the FRP reinforcement is embedded into grooves carved on the concrete substrate. The groove will then be filled with an epoxy resin or a cementitious grout. However, most of the research pertaining to NSM method were focused on strengthening using FRP laminate strips while fewer data are available on strengthening of RC beams with NSM FRP reinforcing bars.

De Lorenzis and Nanni (2001) directed an experimental and analytical study in order to characterize the shear strengthening of RC beams using NSM FRP reinforcing bars. Their experimental campaign was composed of eight full-scale T-beams, six of which were retrofitted. The test variables were internal steel shear reinforcement, FRP bar spacing, retrofitting scheme, end anchorage of FRP bars, and inclination angle of FRP retrofits. It was shown that application of the NSM FRP bars is an effective solution not only in increasing the shear strength, but also in improving the beam ductility. Compared to the control specimen without internal stirrups, the loading capacity of the retrofitted specimens can increase by up to 106%. However, the failure modes of these specimens underlined debonding as a major issue that needs to be precluded in shear strengthening of RC members using NSM FRP bars. In another experimental study, Barros and Dias (2003) evaluated the efficacy of carbon FRP (CFRP) laminates in improving the shear capacity of two series of beams with different heights. Each series was comprised of five specimens; three of them were retrofitted with different retrofitting scheme and the remainders were kept as the control specimens. A part from one control specimens, all specimens were constructed without any internal shear reinforcements. The test parameters were comprised of the beam height (150 mm or 300 mm), type of CFRP retrofits (wet lay-up sheet or pre-cured laminate strip), and

*Corresponding author, Assistant Professor
E-mail: morshed@yazd.ac.ir
[a]M.Sc. Graduate
E-mail: moein_civil87@yahoo.com
[b]Assistant Professor
E-mail: a.eslami@yazd.ac.ir

ISSN: 1225-4568 (Print), 1598-6217 (Online)

inclination angle of CFRP retrofits (45°, 90°). The laminate strips were applied using NSM technique. All specimens were loaded under a four point bending test set-up. The experimental results exhibited a load increase in all retrofitted beams ranged from 22% to 77% compared to the control specimen which contained no transverse reinforcement. In addition, it was confirmed that the NSM laminate strips were more efficient than the wet lay-up sheets in enhancing both the loading capacity and displacement ductility.

Shear strengthening of RC beams using NSM technique has also been experimentally described by Rizzo and De Lorenzis (2009). A total of nine specimens were included in their experimentation. One specimen was left without any strengthening and used as the control specimen, one was retrofitted using externally bonded U-wrap configuration while the rest were strengthened with NSM FRP. All the control and retrofitted specimens were designed to fail in shear. The test variables included strengthening technique, type of NSM FRP (bar or strip), type of groove filler, and spacing and inclination angle of NSM reinforcement. Based on their results, the shear strength of the NSM retrofitted specimens can increase by up to 44.4% compared to the control specimen. In addition, the experimental observations pointed out concrete cover separation of the internal shear reinforcement as the failure mode of all the specimens retrofitted using NSM technique.

In another experimental investigation, Jalali *et al.* (2012) evaluated the effectiveness of NSM technique using an innovative manually made FRP rods for shear strengthening of RC beams. Their study was comprised of six shear deficient RC beams and aimed at precluding the undesirable debonding failure mode of the NSM reinforcement. Their test variables were FRP bar spacing, inclination angle, and end anchorage. According to their results, rang of shear strength increment in the retrofitted specimens was between 22% and 48%. In addition, application of the end anchors could change the failure mode from debonding to diagonal shear cracking followed by concrete cover separation.

From the literature reviewed in the current study, debonding of FRP reinforcing bars can be confirmed as the dominant mode of failure in shear strengthening of RC beams using NSM technique. It is evident that debonding failure typically happens before using the maximum strength of FRP reinforcement. Although limited previous studies have attempted to overcome this issue, more investigations are needed to elaborate on the behavior of RC beams shear strengthened with NSM FRP bars in order to preclude/postpone premature debonding failure and to fully exploit the strength of FRP materials. Towards this, the current study was aimed at accomplishing an optimal state of shear strengthening using NSM GFRP bars. The test variables are GFRP bar spacing and inclination angle, shape of the grooves, and end anchorage.

2. Experimental program

2.1 Specifications of the as-built and retrofitted specimens

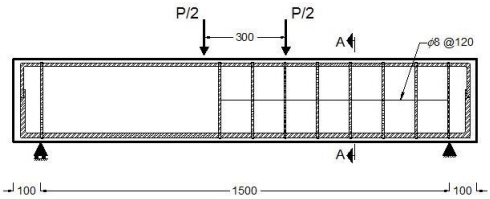

Fig. 1 The geometric dimensions and reinforcement details of the test specimens (all dimensions are in mm)

To achieve the main objectives of this research, a total of six shear deficient RC beams were included in the experimental campaign. All the test specimens were measured 1700 mm in length with a rectangular cross-section of 150×300 mm. The geometry and reinforcement details of the test specimens are schematically illustrated in Fig. 1. A clear concrete cover of 20 mm to the surface of shear reinforcement was incorporated in all specimens. The as-built test specimens were designed to ensure that the dominant failure mechanism would be the shear failure. Towards this, the shear span of each beam in one side was left without any shear reinforcement (hereafter referred to as the weak side) to precipitate the shear failure in this zone. The rest of the beam specimens was detailed with 8 mm diameter rebars spaced at 120 mm to resist all shear forces induced during the experimentation. The longitudinal steel reinforcement consisted of two 18 mm diameter rebars at the bottom as tensile reinforcement and two 12 mm diameter rebars at the top as compressive reinforcement. For retrofitting, only the weak side was strengthened in shear with NSM GFRP rebars.

Out of the total specimens, one was left un-strengthened and used as the control specimen, whereas the weak part of the other five beams were strengthened in shear using NSM GFRP rebars of various schemes. The nominal diameter of the bars used for retrofitting was 4 mm and their surface were treated with helically wrapping to increase their bond strength. The test variables are as follows.

Inclination angle of the NSM reinforcement with respect to the longitudinal axis of the specimens. Two different angles of 90° (vertical reinforcement) and 45° were selected for retrofitting.

Spacing of the NSM GFRP rebars. The selected values measured along the beam axis were 100 mm, 120 mm, and 150 mm.

Groove shapes. The grooves were carved in two different shapes either with a constant or with a variable depth and width along their length (i.e., prismatic and non-prismatic grooves).

Table 1 provides the shear strengthening details of the retrofitted specimens. The test specimens were designated using a mnemonic notations in terms of numbers and letters. The initial letter “B” stands for the beam followed by either NSM FRP spacing along the beam axis (100, 120, 150 mm) or the letter “C” which corresponds to the control specimen. The second and third numbers indicate the groove depth (12, 15 mm) and inclination angle of NSM FRP rebars (45° and 90°), respectively. The letter “M” for the last beam in Table 1 refers to a modified version of NSM GFRP shear reinforcement. The retrofitting details of

Table 1 Details of the test specimens

Specimen	Strengthening system	Groove dimension (mm)			Inclination angle (deg.)
		Depth	Width	Spacing	
BC	None	–	–	–	–
B120-12-90	NSM	12	6	120	90
B100-15-90	NSM	15	6	100	90
B150-15-90	NSM	15	6	150	90
B150-15-45	NSM	15	6	150	45
B120-12-90-M	MNSM	12	6	120	90

specimen B120-12-90-M is similar to specimen B120-12-90 except that the former specimen was retrofitted using an innovative modified NSM (MNSM) configuration in order to preclude undesirable premature debonding of NSM GFRP bars and to exploit all the strength of the FRP materials in NSM shear retrofitting. In this modification, the GFRP bars were manually strengthened by wrapping their ends with externally bonded CFRP sheets while the depth of the grooves at mid-span was remained constant (12 mm).

2.2 Retrofitting procedure

As indicated in Table 1, the adopted strengthening schemes can be classified into two categories; namely NSM and MNSM. For the beams retrofitted with conventional NSM scheme, preparation began by carving prismatic grooves with the specified dimensions using a hand grinder. The grooves were aimed to have a rectangular cross-section with a constant width of approximately 6 mm, corresponding to one and a half of the actual diameter of the GFRP bar as stipulated in ACI 440-08 design code [20], while their depth was different in each beam. After that, they were cleaned using an air jet to remove any particles that may jeopardize the proper bonding of the epoxy adhesive and concrete substrate. Next, the FRP bars were installed into the grooves. The installation procedure was comprised of the partially filling the grooves with the epoxy adhesive, and inserting the bars with a slight pressure to completely fill the space between the bars and grooves. The grooves were subsequently filled with more epoxy adhesive and the excessive adhesive was removed to level their surface. Finally, the retrofitted specimens were cured at room temperature for seven days to ensure that epoxy adhesive had reached its full mechanical properties.

For the specimen retrofitted using MNSM, B120-15-90-M, retrofitting procedure was different from the others. In this modified method, the end parts of the NSM FRP bars were wrapped with externally bonded CFRP sheets. The manufacturing procedure followed the steps shown in Fig. 2. First, a square sheet of CFRP fabrics was cut with a width of around 80 mm and fully saturated with the two component epoxy resin. The manufacturing process was followed by tightly wrapping (about 6 layers) the saturated CFRP strips around the GFRP bars and expelling any air entrapped between CFRP layers by hand. The prepared bars, as shown in Fig. 3, were then cured in room temperature for seven days before being mounted on the

Fig. 2 Manufacturing process of the manually strengthened GFRP bars

Fig. 3 Illustration of the manually strengthened GFRP bars

Fig. 4 Grooves carved for MNSM strengthening method

specimen. In the MNSM strengthening method grooves are slightly different from the NSM method. While the later method contained grooves with a constant rectangular cross-section, grooves in the former method can be divided into three different parts. As observed in Fig. 4, in the MSNM method, both ends of the grooves were the same with a greater cross-section than the middle part to have enough room to place the manually strengthened FRP bars. The middle part was a prismatic groove; 6 mm wide, 12 mm deep, and 140 mm long. At the ends, the width and depth were gradually increased to 15 mm and 30 mm, respectively, to prevent stress concentration. It is worth mentioning that assuming 1 mm thickness for each layer of CFRP wraps, this provided width would be approximately one and a half of the diameter of the manually strengthened part of the GFRP bars following the similar ratio adopted in the middle part and the other retrofitted specimens. Retrofitting procedure using manually strengthened FRP bars was identical to NSM method as explained before.

2.3 Test set-up, instrumentation, and loading

The test specimens were loaded under a four-point

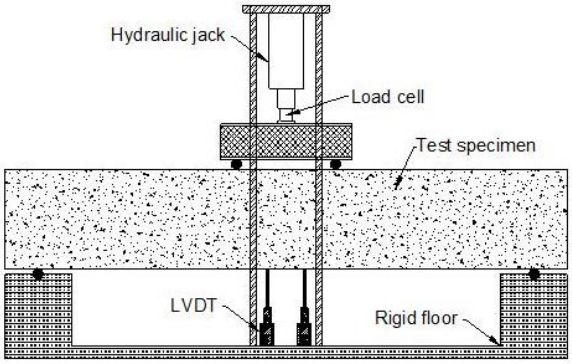

Fig. 5 Schematic illustration of test set-up

Table 2 Mechanical properties of steel reinforcement

Bar diameter (mm)	Stress (MPa)		Elastic Modulus (GPa)
	Yield	Ultimate	
8	538	596	196
12	493	580	203
18	485	573	206

bending configuration as schematically illustrated in Fig. 5. The shear span was measured to be 600 mm for all specimens. Loading was applied in the form of a monotonically increasing load at the mid-span of the specimens using a 5 kN hydraulic jack up to failure while the mid-span displacements were measured using two linear variable displacement transformers (LVDTs). To mark the cracking pattern, the applied load was kept constant for a few moments at the end of each loading step. During the experimentation, the beam mid-span loads and deflections were recorded and used in the analysis.

2.4 Material properties

All the test specimens were cast simultaneously using a normal weight, ready-mix concrete with the maximum aggregate size of 19 mm. The concrete slump was measured to be about 95 mm. The compressive strength of concrete was determined to be about 28.3 MPa by testing cylinder specimens of 150×300 *mm*. The mechanical properties of steel reinforcing bars were obtained using direct tensile tests conforming to ASTM A370 (2017) as summarized in Table 2.

The tensile properties of GFRP bars (4 mm diameter) used as NSM shear retrofits were also determined using coupon tests following the provisions of CSA S806-12 (2012). Towards this, five coupon specimens were prepared as shown in Fig. 6. The length of the steel tube anchor at each side was about 250 mm whilst its inner diameter was around 17 mm. The free length of bar between two tubes was 160 mm (40 times FRP bar diameter) bringing the total length of each specimen to 660 mm. The GFRP bar was aligned with the tube anchors using two plastic rings possessing an outer diameter equal to the inner diameter of the tubes. The tubes were then filled by a non-shrinke cementitious grout and cured for seven days before being tested. Fig. 7 shows one coupon specimen under tensile testing while their obtained properties are provided in Table 3.

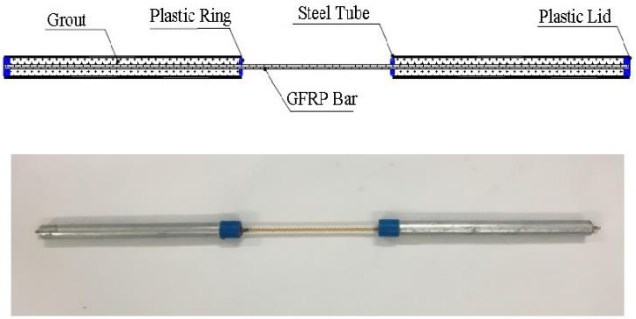

Fig. 6 Details of the GFRP coupon specimens

Fig. 7 Tensile testing of a GFRP bar

Table 3 Tensile properties of GFRP bars

$d_b\,(mm)$	$A_f\,(mm^2)$	E_f (GPa)	f_{fu} (MPa)	ε_{fu}
4	12.56	21	893	0.0458

Table 4 Mechanical properties of epoxy resins

Type	Strength (MPa)			Density (Kg/Lit)
	Bonding	Compressive	Tensile	
EPR301	3.5	95	_	1.65
EPR3301	3.5	95	30	1.5

The unidirectional CFRP sheets used in this study to strengthen NSM GFRP bars has a tensile strength of 4950 MPa, an elastic modulus of 240 GPa, and an ultimate tensile strain of 1.5%. Two types of epoxy resin, EPR301 and EPR3301, were also implemented in the retrofitting procedure. The former was used for embedment of the NSM reinforcing GFRP bars into the grooves whereas the CFRP sheets used in the MNSM method were saturated using EPR3301. Both types have two components, resin and hardener, mixed with a weight ratio of 3:1. The mechanical properties of both types were identical as given in Table 4.

Fig. 8 Cracking pattern and failure mode of the control specimen, BC

Fig. 9 Cracking pattern and failure mode of specimen B120-12-90

3. Experimental results and failure modes

3.1 Specimen BC

Specimen BC was intended to act as a control specimen. As expected, first shear crack was developed in the weak side of the specimen at a load of approximately 95.5 kN and propagates towards the support. At higher loads, this crack widened gradually while narrower cracks were appeared at the weak side, near the support, and below the loading point. Eventually, the beam failed in shear at a load of 111.1 kN while the corresponding mid-span deflection was measured to be approximately 3.3 mm. Fig. 8 shows the failure mechanism of this specimen.

3.2 Specimen B120-12-90

The cracking behavior of specimen B120-12-90 was similar to that of the control beam. Shear cracking was initially appeared at a load of 93.8 kN in the weak side of the beam, underneath the loading point, and propagated with an angle of around 45° towards the bottom. This main crack continuously widened with increasing the load. More shear cracks were also developed around the initial cracks at higher loads. Failure of this beam was attributed to the debonding of NSM GFRP retrofits from the concrete substrate accompanying with cover separation in the vicinity of the support as indicated in Fig. 9. The ultimate loading capacity of the beam and its corresponding mid-span displacement were obtained to be around 171.5 kN and 5.8 mm, respectively.

3.3 Specimen B100-15-90

In this specimen, shear cracks propagated from the loading point towards the support in the weak span at 101.7 kN. With load increment, this crack kept widening up to the failure point. During loading, some minor flexural-shear cracks were also developed around the mid-span and in the strong shear span of the beam. The beam eventually failed in shear at a load of 176.7 kN and mid-span deflection of 9.5 mm. Based on the experimental observations, failure of this specimen was accompanied by debonding and partially rupture of the NSM GFRP retrofits. Fig. 10 indicates the failure mode and cracking pattern of specimen B100-15-90.

Fig. 10 Cracking pattern and failure mode of specimen B100-15-90

Fig. 11 Cracking pattern and failure mode of specimen B150-15-90

3.4 Specimen B150-15-90

During loading of specimen B150-15-90, a major shear crack appeared in the weak span at 109 kN and was subsequently surrounded by more minor ones. In the mid-span, some flexural cracks were also developed and propagated to the mid-height of the specimen. The loading procedure was continued until the premature debonding of NSM GFRP retrofits induced a shear failure as indicated in Fig. 11. The beam failed at a load of 145.6 kN corresponding to a mid-span deflection of 4.9 mm.

3.1.5 Specimen B150-15-45

For specimen B150-15-45, GFRP retrofits were installed with an inclination angle of 45°. The cracking pattern of this specimen was similar to others except a higher distribution of cracks across the weak span. This indicates the efficiency of the inclined shear retrofits in retaining the width of shear cracks. During the test, first flexural-shear crack was started to develop at a load of 141.8 kN. This trend was followed by formation of some flexural cracks at

Fig. 11 Cracking pattern and failure mode of specimen B150-15-45

Fig. 13 Flexural cracking of specimens B120-12-90-M

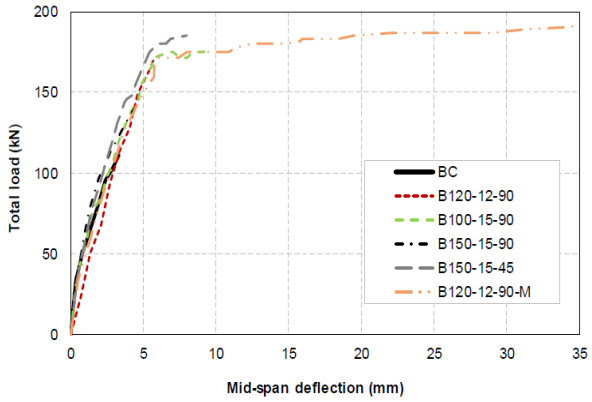

Fig. 14 Distribution of the total load versus mid-span displacement for all the test specimens

the strong span of the beam at approximately 149.1 kN. At a load of 174.9 kN, shear cracks were also observed near the weak side support of the beam and propagated towards the loading point. This beam failed at a load of 185.3 kN and a mid-span deflection of 8.0 mm. Based on the experimental observations, the shear failure mode of this specimen was due to the rupture of NSM GFRP retrofits with partial debonding and cover separation. Fig. 12 provides an illustration of the specimen after failure.

3.6 Specimen B120-12-90-M

The modification adopted for specimen B120-12-90-M could distinguish the structural performance of this specimen compared to others as shown in Fig. 13. During loading, initially flexural cracks were developed at the mid-span of the beam at a load of 119.7 kN. Then, at a load of 137 kN, first shear crack started to extend underneath of the loading point at the weak side of the specimen and continued towards the support. With increasing the load, the flexural cracks widened and propagated within the height of the specimen. At a load of 181.8 kN, more flexural cracks appeared at the strong span. The beam failed at a load of 192.2 kN corresponding to a mid-span deflection of 34.9 mm. Of particular interest was the large deformation of the beam before failure which pointed out a desirable ductile behavior. Failure of the beam was attributed to the concrete crushing under flexure. The NSM FRP retrofits were capable of restraining the width of the shear cracks. However, at the onset of failure, lack of aggregate interlock resulted in the rupture of some FRP bars crossed the shear cracks. Experimental testing of specimen B120-12-90-M confirmed the efficacy of the adopted MNSM retrofitting technique in changing the failure mode of this beam from shear to flexure.

4. Comparison and discussion

The experimental results of the control and retrofitted specimens were compared together in terms of loading capacity, ultimate deformation, displacement ductility, and elastic stiffness. The effects of test parameters including GFRP bar spacing, inclination angle, shape of the grooves, and end anchorage are also elaborated in the following.

4.1 Load carrying, deformation capacity, and elastic stiffness

The variation of the total load applied during the experimentation of each test was plotted against the obtained mid-span deflection and shown in Fig. 14. According to these curves, the initial stiffness of the test beams cannot be significantly affected by the strengthening intervention. However, the loading capacity and ultimate deformation of the retrofitted beams were higher than that of the control specimen. Table 5 provides a numerical comparison of the maximum loading and displacement capacities for all the test specimens. As no internal shear reinforcement was provided for the test specimens, the contribution of the GFRP retrofits in shear capacity can be calculated by subtracting the shear capacity of the retrofitted specimens from the control beam, BC.

Of particular interest was the structural behavior of the specimen retrofitted with the modified NSM technique, B120-12-90-M, compared to the others. The former experienced the greatest increase in the ultimate loading capacity and mid-span displacement. This outstanding and distinguished performance was mainly attributed to the efficiency of the adopted modification in precluding the premature debonding failure of the NSM FRP retrofits changing the failure mode of specimen B120-12-90-M from shear to flexure as observed in Fig. 14. Comparing the four beam specimens strengthened with conventional NSM method, the highest increase in the ultimate loading capacity was measured for specimen B150-15-45 in which the GFRP bars were installed with an inclination of 45°. However, this specimen was still ruptured in shear, similar to the control beam.

4.2 Inclination angle of GFRP bars

Comparing the experimental results of specimens B150-

Table 5 Summary of the test results

Specimen	Maximum total load (kN)	Ultimate displacement (mm)	Shear capacity		
			Maximum (kN)	Increase (%)	Contribution of GFRP retrofits (kN)
BC	111.1	3.3	55.6	_	_
B120-12-90	171.5	5.8	85.8	54	30.2
B100-15-90	176.7	9.5	88.4	59	32.8
B150-15-90	145.6	4.9	72.8	31	17.3
B150-15-45	185.3	8.0	92.7	67	37.1
B120-12-90-M	192.2	34.9	96.1	73	40.6

15-90 and B150-15-45 can explain the influence of inclination angle of GFRP bars in shear retrofitting using NSM technique. Apart from the different inclination angle of the NSM GFRP bars (45° and 90°), all other details of these two specimens were the same. Based on the experimental measurements given in Table 5, changing the inclination angle of GFRP bars from 90° to 45° caused an increase of 27% and 65% in the loading capacity and ultimate mid-span deflection, respectively. This is mainly due the most appropriate direction of the 45° inclined GFRP bars which is approximately perpendicular to the shear crack (aligned with the maximum shear stress). However, it is worth mentioning that this retrofitting configuration cannot be plausible under cyclic loading reversal where the direction of shear forces changes inversely.

4.3 Spacing of GFRP bars

In order to investigate the effect GFRP bar intervals, two specimens (i.e., B100-15-90 and B150-15-90) were constructed with the same groove details but with two different bar spacing (100 and 150 mm). Comparing the experimental results of specimens B100-15-90 and B150-15-90, it can be concluded that increasing the GFRP bar spacing from 100 mm to 150 mm resulted in 21% and 100% decrease in the load carrying capacity and ultimate mid-span deflection, respectively. This finding was anticipated as increasing the bar intervals will reduce the ratio of shear retrofit.

4.4 MNSM vs NSM retrofitting method

The effectiveness of the adopted modification in NSM retrofitting configuration can be evaluated by comparing the results obtained from the experimental tests of specimens B120-12-90 and B120-12-90-M. These two specimens were retrofitted with two different retrofitting techniques (i.e., conventional NSM and MNSM) while their other details remained identical. Their experimental tests pointed out a substantially improvement in the structural behavior of specimen B120-12-90-M compared to its counterpart, confirming the efficiency of the proposed retrofitting modification. A close observation of the results indicated the debonding of GFRP shear retrofit in specimen retrofitted using conventional NSM technique, B120-12-90, leading to a premature shear failure. Implementing the modification in retrofitting configuration, however, prevented this debonding failure and consequently a ductile flexural failure mode was observed for specimen B120-12-90-M. As shown in Fig. 13 and Table 5, the load carrying capacity and ultimate mid-span displacement of specimen B120-12-90-M were respectively 12% and 506% higher than those measured for specimen B120-12-90.

Table 6 Shear contibution ratio of the FRP retrofits bar

Specimen	Contribution of FRP shear retrofits (kN)		α
	Theoretical	Experimental	
B120-12-90	49.2	30.2	0.61
B100-15-90	59.0	32.8	0.56
B150-15-90	39.3	17.3	0.44
B150-15-45	55.6	37.1	0.67
B120-12-90-M	49.2	40.6	0.83

5. Analytical investigation

The contribution of GFRP retrofits in shear capacity of the test specimens can be analytically predicted by

$$V_f = \alpha \frac{A_f f_{fu} d}{s} (\cos\theta_f + \sin\theta_f) \quad (1)$$

where A_f is the cross sectional area of GFRP retrofts, f_{fu} stands for the ruptured tensile strength of GFRP bars, and d is the effective depth of the beam specimen. Also, $\boldsymbol{S}$ and θ_f are the spacing and inclination angle of the GFRP bars to the longitudinal axes of the beam, respectively. In addition, α is a constant factor which indicates the ratio of the actual shear contoribution of GFRP retrofits to the theoritical value. Based on the experimental tests conducted herin, the value of α was calculated for each specimen and given in Table 6. It is worth mentioning that although for specimen B120-12-90-M, the FRP retrofits could change the failure mode of the beam from shear to flexure, loss of the aggregate interlock could lead to rupture of the FRP bars at the onset of failure. Based on the experimental results of the current study, the highest value for factor α was obtained by adopting the MNSM retrofitting technique.

6. Conclusions

This paper described the results of an experimental study on shear strengthening of deficient RC beams using NSM FRP bars. To overcome the undesirable debonding failure, an innovative method called modified NSM (MNSM) technique was also developed and its efficiency was assessed through experimentation. The actual contribution of FRP bars in increasing the shear capacity of the test beams was also determined by introducing a contribution factor. Based on the experimental and analytical investigations, the following main conclusions can be drawn:

1-NSM GFRP reinforcement can significantly improve the shear capacity of RC beams lacking the requisite

strength. For the specimens strengthened with NSM GFRP bars in the current study, the shear capacity could increase from 31% to 66%. However, this increment was measured to be approximately 73 % for the beam strengthened with MNSM method. The use of MNSM GFRP reinforcement was more efficient in terms of precluding premature debonding and exploiting the strength of FRP shear retrofit.

2-Failure of all the specimen strengthened with NSM technique was governed by shear, whereas a ductile flexural failure was observed for the test specimen strengthened with MNSM technique.

3-Adoption of the proposed modification for retrofitting GFRP bars could result in increasing the ultimate displacement capacity of specimen B120-12-90-M, up to more than ten times higher than the control specimen. The load-displacement curve of specimen B120-12-90-M exhibited a distinguished ductile behavior by experiencing displacement values far beyond the yield point of flexural reinforcement. For the other specimens, however, the ultimate displacement was not measured far from the yield point.

It should be noted that these findings relied on the results of the limited specimens tested in the current study and more comprehensive research are needed to reconfirm the outcomes and elaborate on all aspects of the suggested modified approach.

Acknowledgments

The Authors would like to extend their gratitude towards Yazd University for the financial support of this project.

References

ACI Committee 440 (2008), *Guide for the Design and Construction of Externally Bonded FRP Systems for Strengthening Concrete Structures (ACI 440.2R-08)*, Farmington Hills, Michigan, U.S.A.

Anil, O., Belgin, C.M. and Kara, M.E. (2010), "Experimental investigation on CFRP-to-concrete bonded joints across crack", *Struct. Eng. Mech.*, **35**(1), 1-18.

ASTM A370 (2017), *Standard Test Methods and Definitions for Mechanical Testing of Steel Products*, American Society for Testing and Materials, West Conshohocken, Pennsylvania, U.S.A.

Baji, H., Eslami, A. and Ronagh, H.R. (2015), "Development of a nonlinear FE modelling approach for FRP-strengthened RC beam-column connections", *Struct.*, **3**, 272-281.

Barros, J.A. and Dias, S.J. (2003), "Shear strengthening of reinforced concrete beams with laminate strips of CFRP", *Proceedings of the International Conference Composites in Constructions*.

Bianco, V., Monti, G. and Barros, J.A. (2014), "Design formula to evaluate the NSM FRP strips shear strength contribution to a RC beam", *Compos. Part B: Eng.*, **56**, 960-971.

Chajes, M.J., Thomson, T.A., Januszka, T.F. and Finch, W.W. (1994), "Flexural strengthening of concrete beams using externally bonded composite materials", *Constr. Build. Mater.*, **8**(3), 191-201.

CSA (2012), *Design and Construction of Building Structures with Fibre-Reinforced Polymers*, CSA-S806-12, Canadian Standards Association, Mississauga, Ontario, Canada.

Dalalbashi, A., Eslami, A. and Ronagh, H.R. (2012), "Plastic hinge relocation in RC joints as an alternative method of retrofitting using FRP", *Compos. Struct.*, **94**(8), 2433-2439.

Dalalbashi, A., Eslami, A. and Ronagh, H.R. (2013), "Numerical investigation on the hysteretic behavior of RC joints retrofitted with different CFRP configurations", *J. Compos. Constr.*, **17**(3), 371-382.

De Lorenzis, L. and Nanni, A. (2001), "Shear strengthening of reinforced concrete beams with near-surface mounted fiber-reinforced polymer rods", *ACI Struct. J.*, **98**(1), 60-68.

Deng, J., Airong, L., Peiyan, H. and Xiaohong, Z. (2016), "Interfacial mechanical behaviors of RC beams strengthened with FRP", *Struct. Eng. Mech.*, **58**(3), 577-596.

Dias, S.J. and Barros, J.A. (2013), "Shear strengthening of RC beams with NSM CFRP laminates: Experimental research and analytical formulation", *Compos. Struct.*, **99**, 477-490.

El-Mihilmy, M.T. and Tedesco, J.W. (2000), "Analysis of reinforced concrete beams strengthened with FRP laminates", *J. Struct. Eng.*, **126**(6), 684-691.

Eslami, A. and Ronagh, H.R. (2014), "Experimental investigation of an appropriate anchorage system for flange-bonded carbon fiber-reinforced polymers in retrofitted RC beam-column joints", *J. Compos. Constr.*, **18**(4), 04013056.

Jalali, M., Sharbatdar, M.K., Chen, J.F. and Alaee, F.J. (2012), "Shear strengthening of RC beams using innovative manually made NSM FRP bars", *Constr. Build. Mater.*, **36**, 990-1000.

Khalifa, A., Gold, W.J., Nanni, A. and Mi, A.A. (1998), "Contribution of externally bonded FRP to shear capacity of RC flexural members", *J. Compos. Constr.*, **2**(4), 195-202.

Kocak, A. (2015), "Earthquake performance of FRP retrofitting of short columns around band-type windows", *Struct. Eng. Mech.*, **53**(1), 1-16.

Kocak, A., Onal, M.M. and Sonmez, K. (2007), "Repairing and strengthening methods for RC structural members", *Proceedings of the 6th International Conference on Fracture Mechanics of Concrete and Concrete Structures, Volume 2: Design, Assessment and Retrofitting of RC Structures*, Catania, Italy.

Mahini, S.S. and Ronagh, H.R. (2011), "Web-bonded FRPs for relocation of plastic hinges away from the column face in exterior RC joints", *Compos. Struct.*, **93**(10), 2460-2472.

Mahini, S.S. and Ronagh, H.R. (2010), "Strength and ductility of FRP web-bonded RC beams for the assessment of retrofitted beam-column joints", *Compos. Struct.*, **92**(6), 1325-1332.

Mosallam, A.S. and Banerjee, S. (2007), "Shear enhancement of reinforced concrete beams strengthened with FRP composite laminates", *Compos. Part B-Eng.*, **38**(5-6), 781-793.

Mostofinejad, D. and Mahmoudabadi, E. (2010), "Grooving as alternative method of surface preparation to postpone debonding of FRP laminates in concrete beams", *J. Compos. Constr.*, **14**(6), 804-811.

Onal, M.M., Zengin, B., Kocak, A. and Doran, B. (2014), "An experimental investigation on flexural behavior of RC beams strengthened with different techniques", *KSCE J. Civil Eng.*, **18**(7), 2162-2169.

Rizzo, A. and De Lorenzis, L. (2009), "Behavior and capacity of RC beams strengthened in shear with NSM FRP reinforcement", *Constr. Build. Mater.*, **23**(4), 1555-1567.

Teng, J., Huang, Y., Lam, L. and Ye, L. (2007), "Theoretical model for fiber-reinforced polymer-confined concrete", *J. Compos. Constr.*, **11**(2), 201-210.

PL